NEUROSCIENCE

# Pathogenic tau–induced transposable element–derived dsRNA drives neuroinflammation

**Elizabeth Ochoa[1,2,3], Paulino Ramirez[1,2,3], Elias Gonzalez[1,2,3], Jasmine De Mange[1,2,3], William J. Ray[4], Kevin F. Bieniek[2,5], Bess Frost[1,2,3]***



**Deposition of tau protein aggregates in the brain of affected individuals is a defining feature of "tauopathies," including Alzheimer's disease. Studies of human brain tissue and various model systems of tauopathy report that toxic forms of tau negatively affect nuclear and genomic architecture, identifying pathogenic tau–induced heterochromatin decondensation and consequent retrotransposon activation as a causal mediator of neurodegeneration. On the basis of their similarity to retroviruses, retrotransposons drive neuroinflammation via toxic intermediates, including double-stranded RNA (dsRNA). We find that dsRNA and dsRNA sensing machinery are elevated in astrocytes of postmortem brain tissue from patients with Alzheimer's disease and progressive supranuclear palsy and in brains of tau transgenic mice. Using a *Drosophila* model of tauopathy, we identify specific tau-induced retrotransposons that form dsRNA and find that pathogenic tau and heterochromatin decondensation causally drive dsRNA-mediated neurodegeneration and neuroinflammation. Our study suggests that pathogenic tau–induced heterochromatin decondensation and retrotransposon activation cause elevation of inflammatory, transposable element–derived dsRNA in the adult brain.**

## INTRODUCTION

Retrotransposons account for 35% of the human genome (*1*). Fully intact, autonomous retrotransposons mobilize within a host genome via a "copy-and-paste" mechanism involving transcription of retrotransposon DNA, translation of the nascent retrotransposon RNA transcript into proteins, reverse transcription of retrotransposon RNA into DNA using retrotransposon-encoded proteins, and subsequent insertion of the new retrotransposon DNA into a new location in the genome [Fig. 1A, example of a long-terminal repeat (LTR) retrotransposon]. In addition to the mutagenic potential of a mobilization-competent retrotransposon, retrotransposon-induced toxicity can also arise from (i) retrotransposon RNA, (ii) retrotransposon-encoded protein, (iii) retrotransposon-derived double-stranded RNA (dsRNA), (iv) episomal retrotransposon complementary DNA (cDNA), and (v) DNA damage from failed genomic retrotransposon integration events (Fig. 1B) (*2*, *3*).

Multiple recent studies suggest that retrotransposons are activated in the context of tau-mediated neurotoxicity and are a causal factor driving neurodegeneration (*4*–*7*). Retrotransposons that are elevated at the RNA level have been identified in *Drosophila*, mouse, and human tauopathy (*4*–*7*). Retrotransposon-encoded proteins and increased retrotransposon DNA copy number are also elevated in brains of tau transgenic mice (*5*), indicating that retrotransposon RNA is translated and that retrotransposon RNA is actively reverse-transcribed into cDNA. Studies in tau transgenic *Drosophila* report an increase in somatic neuronal retrotransposition events, a process that is amenable to pharmacological intervention via a reverse transcriptase inhibitor (*6*). Mechanistically, pathogenic forms of tau disrupt transcriptional (heterochromatin-mediated) and posttranscriptional [piwi-interacting RNA (piRNA)–mediated] retrotransposon silencing (*6*). While retrotransposons are known to drive inflammation in other human disorders (*1*, *8*–*11*) and studies in the tauopathy field clearly suggest that pathogenic forms of tau activate retrotransposons across model systems, it is currently unknown whether tau-induced retrotransposon activation contributes to neuroinflammation.

In the current study, we sought to determine whether retrotransposon-derived dsRNA is elevated in tauopathy, whether elevation of dsRNA results from failed heterochromatin and/or piRNA-mediated silencing, and whether retrotransposon activation drives neuroinflammation. We find that dsRNA and dsRNA sensing machinery are significantly elevated in astrocytes of postmortem human brain tissue from human patients with Alzheimer's disease or progressive supranuclear palsy (PSP), a "primary" tauopathy, and in brains of rTg4510 tau transgenic mice. Similarly, we find that dsRNA accumulates in astrocyte-like glia of tau transgenic *Drosophila*. We further leverage the *Drosophila* system to identify specific retrotransposons that form dsRNA in the context of tauopathy, to establish that dsRNA causally drives neurodegeneration and activation of an innate immune response, and to discover that deficits in heterochromatin-mediated retrotransposon silencing are sufficient to elevate overall levels of dsRNA and activate the innate immune response.

## RESULTS

### dsRNA and dsRNA-sensing machinery are elevated in astrocytes of human tauopathy

Initial, intermediate, and late phases of Alzheimer's disease are neuropathologically defined via Braak staging, which is based on the degree of neurofibrillary tau pathology in specific areas of the brain (*12*). As we have previously identified retrotransposons that are elevated in postmortem human Alzheimer's disease brain (*6*)

[1]Sam and Ann Barshop Institute for Longevity and Aging Studies, San Antonio, TX, USA. [2]Glenn Biggs Institute for Alzheimer's and Neurodegenerative Diseases, San Antonio, TX, USA. [3]Department of Cell Systems and Anatomy, University of Texas Health San Antonio, San Antonio, TX, USA. [4]The Neurodegeneration Consortium, Therapeutics Discovery Division, University of Texas MD Anderson Cancer Center, Houston, TX, USA. [5]Department of Pathology and Laboratory Medicine, University of Texas Health San Antonio, San Antonio, TX, USA.
*Corresponding author. Email: bfrost@uthscsa.edu

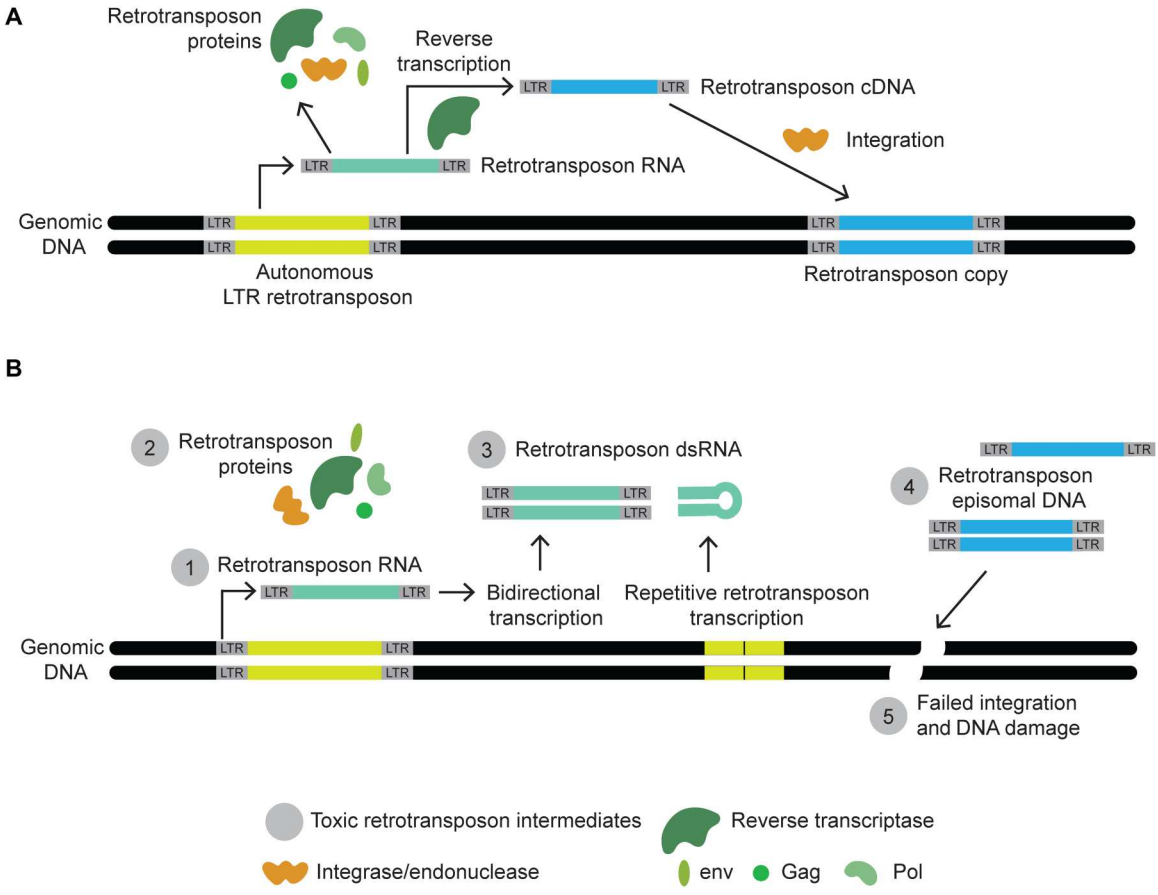


**Fig. 1. Retrotransposon lifecycle and toxicity.** (**A**) Retrotransposons mobilize via a copy-and-paste mechanism, where activation of retrotransposons within genomic DNA involves transcription of retrotransposon RNA, reverse transcription into cDNA, and insertion into a new location within the genome. Depending on the subclass of retrotransposon, the element may encode for proteins needed to facilitate the copy-and-paste mechanism, such as capsid, protease, reverse transcriptase, integrase, and envelope proteins (*2*). (**B**) While retrotransposition can create novel insertions, toxicity can also result from (i) retrotransposon RNA, (ii) retrotransposon proteins, (iii) dsRNA generated from nascent retrotransposon transcripts, (iv) episomal retrotransposon DNA, and (v) DNA double-strand breaks from failed retrotransposon insertions.

and retrotransposons are known to form dsRNA in other human disorders (*8*), we first determined whether the presence of dsRNA correlates with the degree of pathogenic tau burden in the human brain. To quantify the overall dsRNA levels in human brain tissue at Braak stages 0, II/III and V/VI, we used an antibody (J2) that recognizes dsRNA of 40 nucleotides or longer in a non–sequence-specific manner (*13*). To determine whether dsRNA enrichment occurs in a primary tauopathy, we also performed J2 staining in postmortem brains of patients with PSP (table S1). We detect a significant increase in overall levels of dsRNA in brains harboring pathogenic forms of tau compared to controls (Fig. 2, A and B). Among tau-affected brains, we noticed a pattern of J2 enrichment that appeared to be astrocytic. Costaining of brains with antibodies detecting astrocyte-specific glial fibrillary acidic protein (GFAP) and dsRNA reveals significant enrichment of dsRNA in astrocytes of brains affected by tauopathy (Fig. 2, C and D). Additional costaining of brains with the neuron-specific antibody microtubule-associated protein 2 (MAP2) revealed no significant enrichment of dsRNA in neurons of tau-affected brains (fig. S1, A and B). While costaining human brain tissue with antibodies detecting J2 and the microglia-specific antibody ionized calcium binding adaptor molecule 1 (Iba1) revealed the presence of dsRNA in some microglia, quantification of these data indicated an overall lack of dsRNA enrichment in microglia of tau-affected brains compared to control, except in the case of late-stage human Alzheimer's disease (fig. S1, C and D).

As dsRNA are a potent pathogen-associated molecular pattern sufficient to induce an interferon response, we next determined whether melanoma differentiation–associated protein 5 (MDA5) is elevated in tau-affected human brains. MDA5 is a dsRNA helicase in the retinoic acid–inducible gene I–like (RIG-I) receptor family that detects long dsRNA via its DEAD box domain as part of the antiviral innate immune response (*14*, *15*). Costaining of postmortem human brain with antibodies detecting MDA5 and GFAP reveals a significant elevation of MDA5 in astrocytes of tau-affected brains (Fig. 2, E and F). Together, these findings point toward an astrocytic increase in dsRNA and dsRNA surveillance machinery in the context of primary and secondary tauopathy.

## dsRNA and dsRNA sensing machinery are elevated in astrocytes of rTg4510 tau transgenic mice

Having found that dsRNA is elevated in human tauopathy, we next investigated dsRNA accumulation in brains of tau transgenic mice. The rTg4510 mouse model features overexpression of a disease-

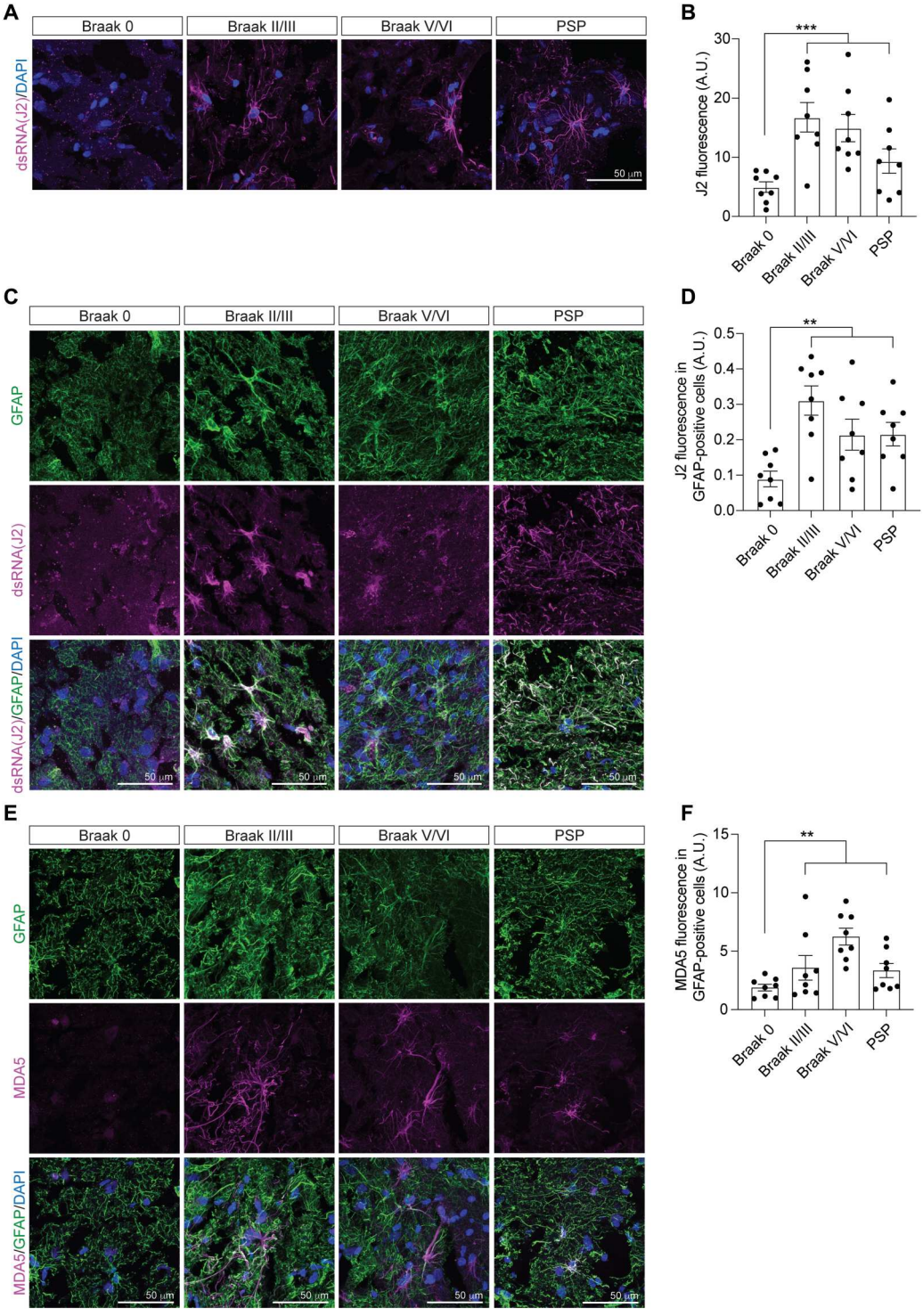


**Fig. 2. dsRNA and dsRNA-sensing machinery are elevated in human tauopathy and localize to astrocytes.** (**A**) Visualization of dsRNA in postmortem human frontal cortex via J2 immunostaining. DAPI, 4′,6-diamidino-2-phenylindole. (**B**) Quantification of (A). A.U., arbitrary units. (**C**) Visualization of dsRNA and astrocytes in postmortem human frontal cortex via J2 and GFAP coimmunostaining. (**D**) Quantification of (C); J2 fluorescence within GFAP-positive cells. (**E**) Visualization of MDA5 and astrocytes in postmortem human frontal cortex via MDA5 and GFAP coimmunostaining. (**F**) Quantification of (E); MDA5 fluorescence within GFAP-positive cells. Scale bars, 50 µm. $n = 8$ biological replicates. $^{**}P < 0.01$; $^{***}P < 0.001$, one-way analysis of variance (ANOVA). Braak 0, little to no detectable pathological forms of tau in the entorhinal region; Braak II/III, pathological forms of tau detected in the entorhinal region as far as the occipitotemporal gyrus; Braak V/VI, pathological forms of tau detected in the entorhinal region extending into the occipital lobe and neocortex. Human cases are described in table S1.

associated (*16*) mutant form of human tau, tau$^{P301L}$, under control of the *Camk2a* promoter (*17*, *18*). rTg4510 mice recapitulate aspects of human tauopathy including but not limited to gliosis, neuronal loss, tau tangle formation, and transposable element activation (*17*–*20*). Using J2-based immunofluorescence, we find a significant elevation of dsRNA in the frontal cortex of tau transgenic mice compared to controls at 6 months of age (Fig. 3, A and B). On the basis of our finding that dsRNA is particularly enriched in astrocytes in human tauopathy, we analyzed dsRNA burden in astrocytes of tau transgenic mice by costaining brains with antibodies detecting dsRNA and astrocytes. Similar to our analyses in human tauopathy, we find a significant increase of dsRNA in astrocytes (Fig. 3, C to E) but not microglia (fig. S2, A to C) or neurons (fig. S2, D and E) in brains of tau transgenic mice aged 6 months compared to control. Having also found increased levels of the dsRNA sensor MDA5 in astrocytes of human tauopathy, we analyzed astrocytic MDA5 in tau transgenic mice. Again, we find a significant elevation of MDA5 in astrocytes of tau transgenic mice aged 6 months (Fig. 3, F to H). Similarly, we detect a significant elevation of overall levels of dsRNA and astrocytic dsRNA in brains of rTg4510 aged 12 months (fig. S3, A to C), along with significantly elevated levels of total MDA5 and astrocytic MDA5 (fig. S3, D to F).

As gliosis begins as early as 2 months in the rTg4510 model (*19*–*21*), we extended our analyses of dsRNA and dsRNA sensing

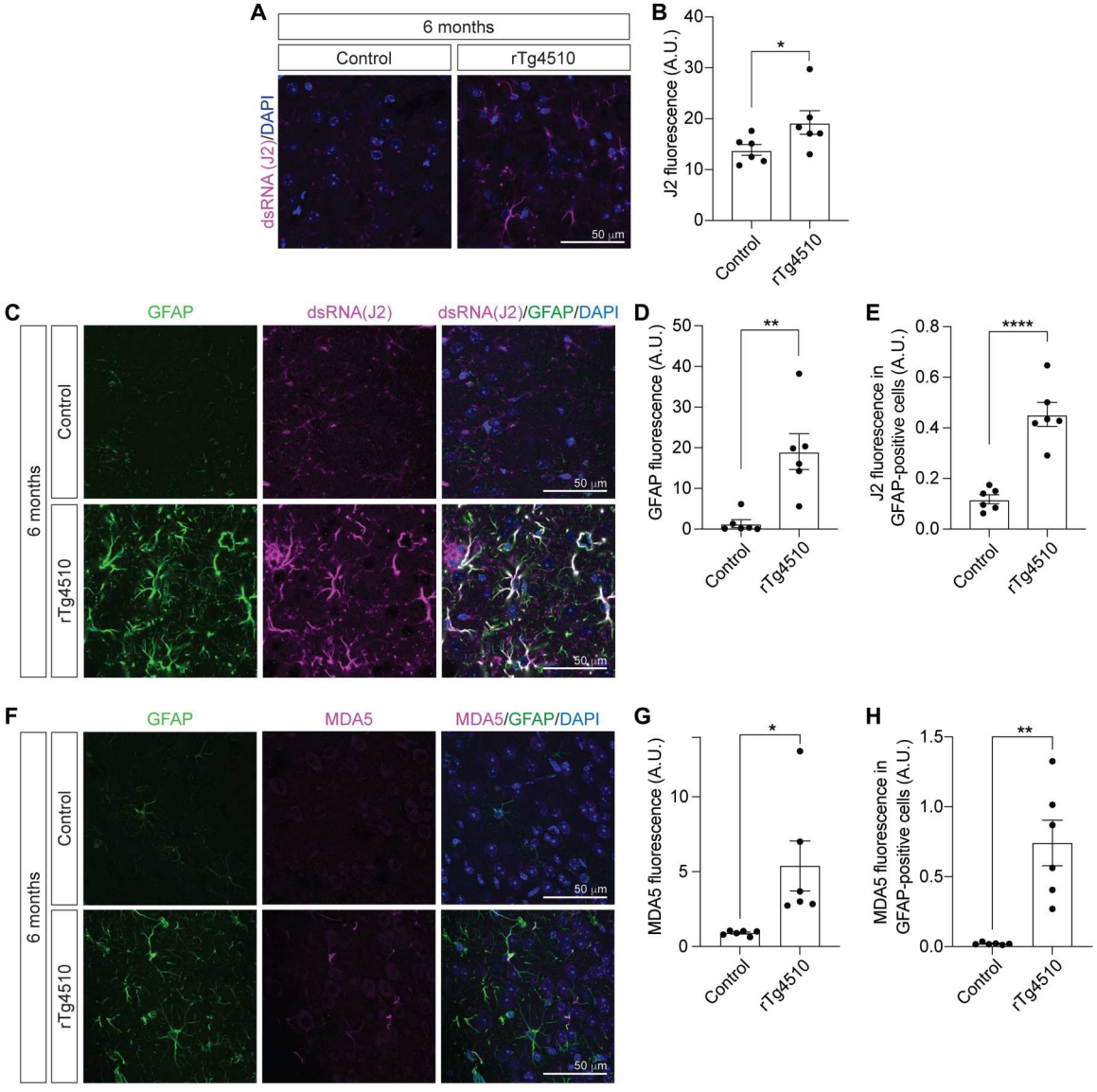


**Fig. 3. dsRNA and dsRNA sensing machinery are elevated in astrocytes of the rTg4510 mouse model of tauopathy at 6 months.** (**A**) Immunofluorescence-based detection of dsRNA in cortex of control and rTg4510 mice using the J2 antibody. (**B**) Quantification of (A). (**C**) Immunofluorescence-based detection of dsRNA and astrocytes (GFAP) in control and rTg4510 mouse cortex. (**D**) Quantification of GFAP-positive astrocytes in (C). (**E**) Quantification of the co-occurrence of dsRNA and GFAP in GFAP-positive astrocytes in control and rTg4510 mouse cortex. (**F**) Immunofluorescence-based detection of MDA5 and astrocytes in control and rTg4510 mouse cortex. (**G**) Quantification of MDA5 in (F). (**H**) Quantification of the co-occurrence of MDA5 and GFAP in GFAP-positive astrocytes in control and rTg4510 mouse cortex. All mice were aged 6 months. Scale bars, 50 µm. $n = 6$ biological replicates. *$P < 0.05$; **$P < 0.01$; ****$P < 0.0001$, unpaired $t$ test.

machinery to control and rTg4510 mice aged 2 months. While 2-month-old rTg4510 mice do not have significantly elevated levels of dsRNA or astrocytic dsRNA compared to controls (fig. S4, A to C), we detect significant elevation of MDA5 in astrocytes of rTg4510 mice at 2 months (fig. S4, D to F). Similar to our findings in human tauopathy, overall levels of dsRNA are unchanged in microglia (fig. S4, G to I) or neurons (fig. S4, J and K) of rTg4510 mice compared to control at 2 months of age. Together, these data indicate that the presence of pathogenic tau is sufficient to drive elevation of dsRNA and dsRNA sensing machinery in the mouse brain in an age-dependent manner. In addition, these data suggest that the astrocytic elevation of dsRNA and MDA5 detected in human Alzheimer′s disease and PSP is a consequence of pathogenic tau.

### Tau-induced elevation of dsRNA mediates neurodegeneration in the adult *Drosophila* brain

To investigate mechanistic links among tau, retrotransposons, dsRNA, and neurodegeneration, we turned to a well-described *Drosophila* model of tauopathy (*22*, *23*). This model is based on pan-neuronal transgenic expression of human tau harboring the human disease-associated (*16*) *R406W* mutation, tau$^{R406W}$ (hereafter referred to as "tau transgenic *Drosophila*") (*22*). We first determined whether elevation of dsRNA observed in human and mouse tauopathy is conserved in brains of tau transgenic *Drosophila.* We used flies at day 10 of adulthood, an age at which a moderate level of neurodegeneration can be detected in this model but before exponential decline in survivorship (*22*, *24*). To quantify overall levels of dsRNA in brains of tau transgenic *Drosophila*, we performed an enzyme-linked immunosorbent assay (ELISA) using anti-dsRNA antibodies J2 and K2. The K2 antibody is a mouse immunoglobulin M (IgM) counterpart to J2 that also detects dsRNA species of 40 nucleotides or greater (*13*). ELISA-based quantification of dsRNA reveals a significant increase in total head lysates of tau transgenic *Drosophila* compared to controls (Fig. 4A). Similarly, we observe overall higher levels of dsRNA in brains of tau transgenic *Drosophila* compared to control based on J2 immunofluorescence (Fig. 4, B and C).

To determine the cell types harboring dsRNA in brains of tau transgenic *Drosophila*, we costained control and tau transgenic *Drosophila* brains with antibodies detecting either elav (neurons) or repo (glia) and dsRNA. While we detect dsRNA in elav-positive neurons (Fig. 4D) and in repo-positive glia (Fig. 4E) of tau transgenic brains, presence of dsRNA in glia appeared to be more abundant than in neurons. *Drosophila* harbor several types of glia, including but not limited to ensheathing glia, cortex glia, and astrocyte-like glia (*25*, *26*), all of which express repo. *Drosophila* astrocyte-like glia are similar to mouse and human astrocytes in that they provide trophic support to neurons (*25*, *27*). In *Drosophila*, astrocyte-like glia can be differentiated from other types of glia by their distinct morphology (*25*, *28*, *29*). On the basis of morphological analysis of repo-positive cells, we find that dsRNA is enriched in astrocyte-like glia of tau transgenic *Drosophila* (Fig. 4F). As the elav protein is restricted to the nucleus, while dsRNA is predominantly cytoplasmic and thus cannot be confidently assigned to a particular nucleus, we did not quantify overall levels of neuronal dsRNA in brains of tau transgenic *Drosophila*.

Having found an increase of the dsRNA sensor MDA5 in both human and mouse tau-affected brains, we next determined whether increasing the detection and clearance of dsRNA ameliorates dsRNA elevation and neurotoxicity in tau transgenic *Drosophila*. While vertebrate systems have several mechanisms of dsRNA detection and clearance, the recognition and clearance of long dsRNA is completed by Dicer-2 in *Drosophila* (*30*). Dicer-2 is a dsRNA-specific endonuclease of the ribonuclease (RNase) III family that cleaves long dsRNA into smaller fragments during RNA interference (RNAi), particularly in the context of viral infection. While *Drosophila Dicer-2* is not a direct homolog of human *MDA5*, both are equipped with DEAD box helicase function (*31*). On the basis of the conserved dsRNA detection and helicase activity between MDA5 and Dicer-2, we determined whether pan-neuronal overexpression of *Dicer-2* was sufficient to decrease dsRNA levels in tau transgenic *Drosophila.* We find that pan-neuronal expression of *Dicer-2* significantly decreases dsRNA levels in tau transgenic *Drosophila* compared to tau expressed alone (Fig. 4G). In addition, terminal deoxynucleotidyl transferase–mediated deoxyuridine triphosphate nick end labeling (TUNEL) reveals that overexpression of *Dicer-2* is sufficient to reduce neurodegeneration in tau transgenic *Drosophila* (Fig. 4H), suggesting that the tau-induced increase in dsRNA causally mediates neurotoxicity. Together, these data indicate that pathogenic forms of tau cause an elevation of dsRNA in astrocytes of human, mouse, and *Drosophila* tauopathy and that dsRNA elevation occurs in the context of toxic forms of wild-type tau (Alzheimer′s disease and PSP) and from mutations in the microtubule-associated protein tau (*MAPT*) gene that cause familial forms of frontotemporal dementia (FTD) [rTg4510 mice (*P301L*) and tau transgenic *Drosophila* (*R406W*)].

### Retrotransposons form dsRNA in brains of tau transgenic *Drosophila*

We have previously identified retrotransposon transcripts that are elevated in tau transgenic *Drosophila* and have developed and validated a custom NanoString code set consisting of probes that recognize these elements (*6*). Having found that dsRNA elevation is conserved among human, mouse, and fly tauopathy, we next leveraged the *Drosophila* system to identify retrotransposons that form dsRNA species. We first immunoprecipitated dsRNA from heads of control and tau transgenic *Drosophila* using the J2 antibody and confirmed the specificity of the J2 antibody for dsRNA via immunoprecipitation with a mouse IgG2A isotype control (fig. S5A). We then quantified retrotransposon transcripts in J2-immunoprecipitated dsRNA relative to total RNA (input) using our custom NanoString retrotransposon code set. We detect an overall trend toward increased retrotransposon-derived dsRNA in tau transgenic *Drosophila*, with a modest but statistically significant increase in *1731{}2219* and *Het-A{}6270*, alongside a robust elevation of *Tabor{}77* (Fig. 5, A and B, and fig. S5B). Together, these data support a model in which pathogenic tau induces formation of retrotransposon-derived dsRNA.

### Loss of heterochromatin-mediated transcriptional silencing is sufficient to increase dsRNA production in the *Drosophila* brain

Having found that dsRNA causally mediate neurodegeneration and identified retrotransposons that form dsRNA in tau transgenic *Drosophila*, we next investigated cellular mechanisms that might underlie tau-induced dsRNA formation. We have previously reported that pan-neuronal expression of human tau in *Drosophila* disrupts two arms of transposable element control: heterochromatin-mediated

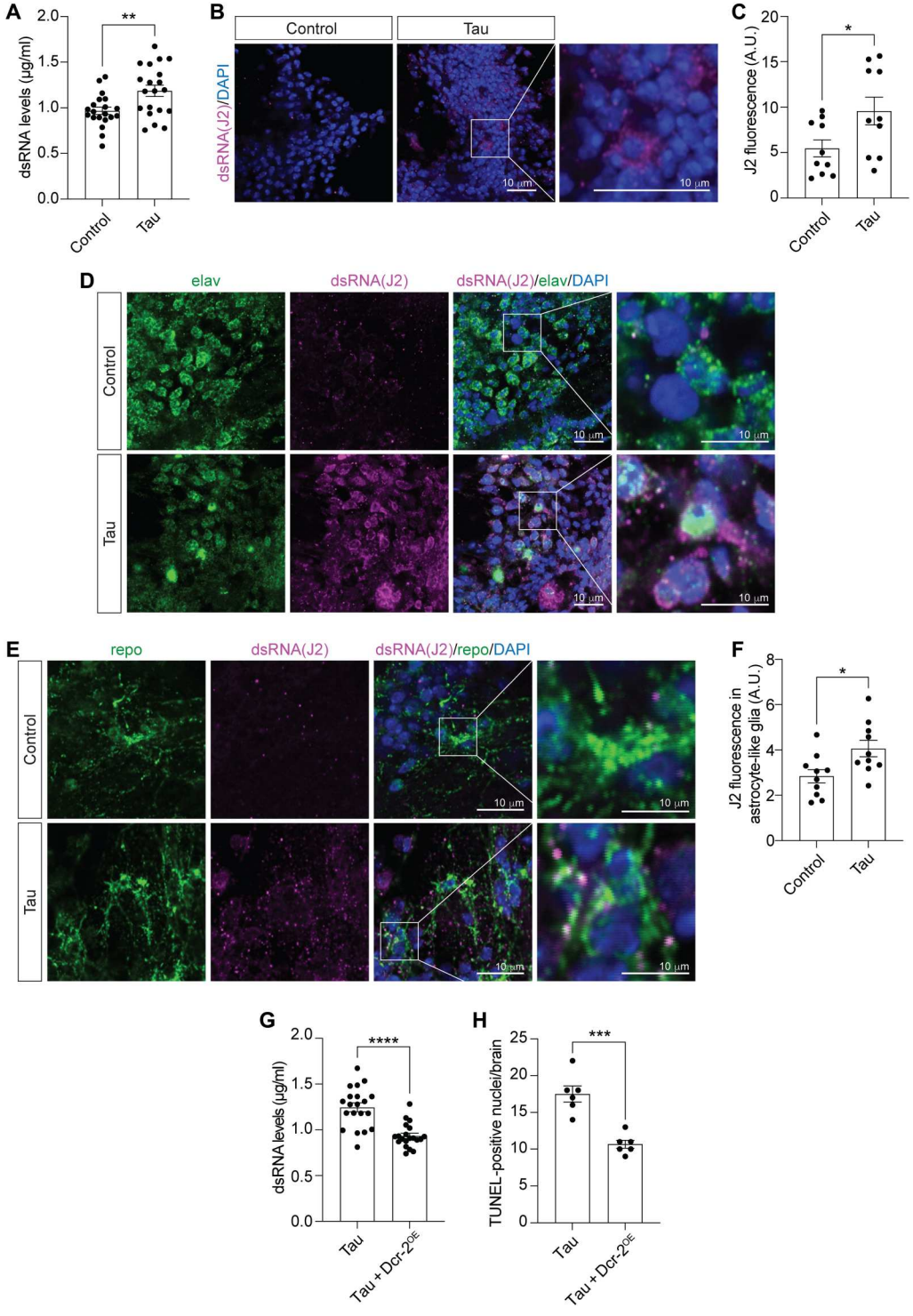


**Fig. 4. dsRNA is elevated in neurons and astrocyte-like glia of tau transgenic *Drosophila* and causally mediates neurotoxicity.** (**A**) J2/K2 ELISA-based quantification of dsRNA levels in heads of control and tau transgenic *Drosophila*. (**B**) Immunofluorescence-based detection of dsRNA in control and tau transgenic *Drosophila* using the J2 antibody. (**C**) Quantification of (B). (**D**) Localization of dsRNA in elav-positive neurons in control and tau transgenic *Drosophila*. (**E**) Localization of dsRNA in repo-positive astrocyte-like glia in control and tau transgenic *Drosophila*. (**F**) Quantification of (E). (**G**) ELISA-based quantification of dsRNA in heads of tau transgenic *Drosophila* and tau transgenic *Drosophila* with genetic pan-neuronal overexpression of *Dicer-2* (Tau+Dcr-2$^{OE}$). (**H**) TUNEL-based quantification of neurodegeneration in brains of tau transgenic *Drosophila* and tau transgenic *Drosophila* with genetic pan-neuronal overexpression of *Dicer-2*. All experiments were performed at 10 days of adulthood; $n = 20$ biological replicates for (A) and (G), where each replicate consists of total RNA lysates from six pooled heads analyzed in triplicate. $n = 10$ biological replicates in (B) to (F); $n = 6$ biological replicates for (H). Scale bars, 10 µm. *$P < 0.05$; **$P < 0.01$; ***$P < 0.001$; ****$P < 0.0001$, unpaired *t* test.

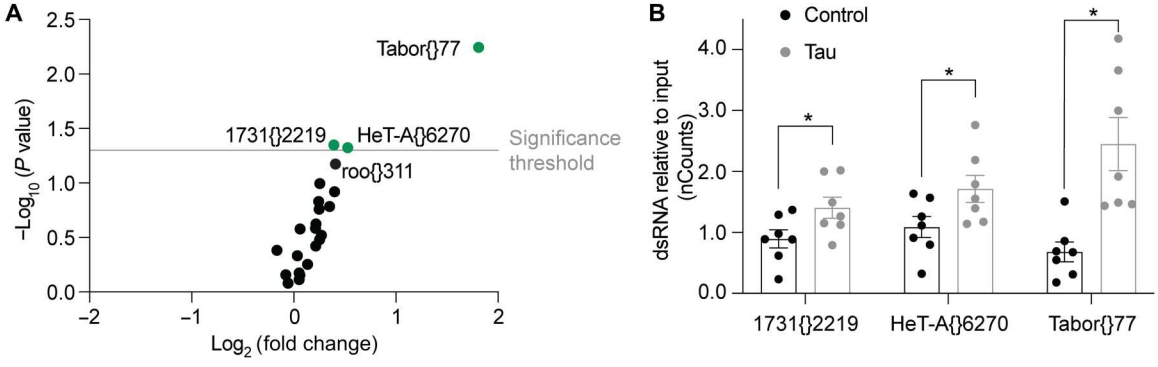


**Fig. 5. Identification of retrotransposons that form dsRNA in brains of tau transgenic *Drosophila*.** (**A**) NanoString-based quantification of retrotransposon transcripts in J2-immunoprecipitated RNA relative to input. Each dot is a retrotransposon. A positive $\log_2$ fold change (*x* axis) indicates increased dsRNA formation of that retrotransposon in tau transgenic *Drosophila*. For retrotransposons that are significantly enriched in the dsRNA fraction ($-\log_{10}$ of $P < 0.05$, labeled in green), individual NanoString nCounter counts per sample are provided in (**B**). $n = 7$ biological samples; each sample is composed of five female and five male heads at day 10 of adulthood. Code set probe sequences are included in table S2. $^*P < 0.05$, multiple unpaired two-sample *t* test with Welch correction.

silencing of retrotransposon transcription and piRNA-mediated posttranscriptional degradation of retrotransposon RNA (*6*). Genetic rescue of tau-induced deficits in heterochromatin silencing and piRNA-mediated retrotransposon silencing decrease retrotransposon transcript levels and suppress tau-induced neurotoxicity (*6*, *24*).

To determine whether heterochromatin decondensation is sufficient to elevate dsRNA in the adult *Drosophila* brain, we quantified dsRNA in heads of *Drosophila* with pan-neuronal RNAi-mediated depletion of *Su(var)205* or *Su(var)3-9*. *Su(var)205* encodes heterochromatin protein 1 (HP1) (*32*), while *Su(var)3-9* encodes a histone methyltransferase responsible for adding silencing methyl groups to lysine-9 of histone-3 (*33*). J2/K2 ELISA indicates that pan-neuronal RNAi-mediated depletion of these heterochromatin regulators is sufficient to elevate dsRNA in the fly brain (Fig. 6, A and B). We additionally quantified dsRNA in heads of *Drosophila* with pan-neuronal RNAi-mediated depletion of *rhino*, a fly ortholog of HP1 (*34*, *35*). As rhino is most well known for its role in the germ line, we first confirmed that *rhino* RNA could be detected in total brain lysates and that pan-neuronal RNAi-mediated knockdown of *rhino* significantly depletes *rhino* transcript levels (fig. S6A). Again, J2/K2 ELISA indicates that pan-neuronal knockdown of *rhino* is sufficient to elevate dsRNA in total head lysates (Fig. 6C). Similar to previous studies in which pan-neuronal knockdown of *Su(var)205* or *Su(var)3-9* is sufficient to drive neurodegeneration (*6*), we find that pan-neuronal RNAi-mediated reduction of *rhino* is sufficient to drive neurodegeneration in the adult *Drosophila* brain based on TUNEL (fig. S6B).

We next quantified dsRNA in heads of *Drosophila* with genetic disruption of factors that are critical for piRNA biogenesis. We find that pan-neuronal RNAi-mediated reduction of *piwi* or *aubergine* (*aub*) is insufficient to significantly elevate dsRNA in the adult *Drosophila* brain (Fig. 6, D and E). *Drosophila* carrying a loss-of-function mutation in *Argonaute 3* (*AGO3*), however, has significantly elevated levels of dsRNA (Fig. 6F). Together, these data suggest that loss of heterochromatin-mediated silencing is causal for increased dsRNA production and that loss of piRNA-mediated posttranscriptional retrotransposon silencing likely plays a more minor role in dsRNA regulation.

## Pathogenic tau and loss of heterochromatin silencing are sufficient to induce neuroinflammation

On the basis of mechanistic links between dsRNA and the innate immune response in other human disorders (*36*, *37*), we next determined whether dsRNA formation is a causal factor driving neuroinflammation. We designed a custom NanoString code set consisting of probes that detect an array of RNAs related to the three major immune responses in *Drosophila* including the Toll, immune deficiency (IMD), and Janus kinase (Jak)/signal transducer and activator of transcription (STAT) pathways as well as three genes associated with RNAi (Fig. 7A and tables S3 and S4). When compared to control, we find that pan-neuronal expression of mutant human tau elevates transcripts of innate immune genes across the Toll, IMD, and Jak/Stat pathways (Fig. 7B). In all three pathways, we observe a trend toward increased antimicrobial peptide expression, an indicator of persistent immune activation. In addition, we find elevated transcript levels of the Jak/STAT ligand *upd1* and decreased transcript levels of transcription factor *Stat92E*. Furthermore, we also find that transcripts of the Jak/STAT-regulated gene *vir-1* are elevated in tau transgenic *Drosophila*, indicating activation of the Jak/STAT response. In the RNAi-mediated response to viral nucleic acids in *Drosophila*, AGO2 loads small dsRNA species onto the RNA-induced silencing complex immediately following Dicer-2–dependent degradation of long dsRNA (*38*). We find that transcript levels of *AGO2* are significantly decreased in tau transgenic flies compared to control, suggesting a dysfunctional response to dsRNA. On the basis of our discovery that overexpression of *Dicer-2* is sufficient to reduce dsRNA levels and decrease tau-induced neurotoxicity, we quantified changes to tau-induced neuroinflammation in tau transgenic flies pan-neuronally overexpressing *Dicer-2*. Among significant reduction of various other transcripts associated with innate immune activation (Fig. 7C), tau transgenic *Drosophila* overexpressing *Dicer-2* have reduced transcript levels of the Toll pathway receptor *Toll*, the IMD pathway gene *Fadd*, and the Jak/STAT-regulated gene *vir-1*, suggesting that tau-induced formation of dsRNA is a causal factor driving innate immune activation in the *Drosophila* brain.

With the knowledge that tau drives heterochromatin decondensation in the *Drosophila* brain and that pan-neuronal heterochromatin decondensation activates transposable elements (*6*) and

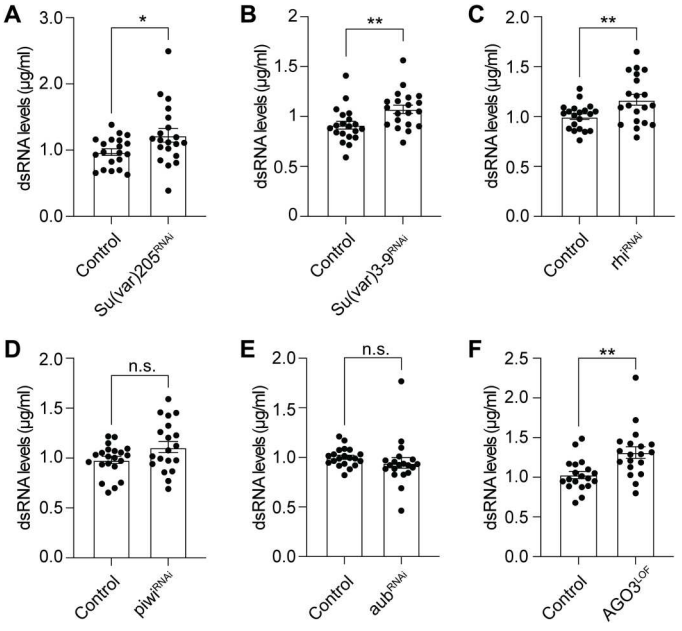


**Fig. 6. Pan-neuronal expression of heterochromatin decondensation is sufficient to elevate dsRNA levels in the *Drosophila* brain.** J2/K2 ELISA-based quantification of dsRNA levels in control and *Drosophila* with pan-neuronal RNAi-mediated reduction or loss of function of (**A**) *Su(var)205*, (**B**) *Su(var)3-9*, (**C**) *rhino*, (**D**) *piwi*, (**E**) *aubergine*, and (**F**) *Argonaute 3*. All experiments were performed in heads of 10-day-old adult flies; $n = 20$ biological replicates, each biological replicate is a pool of three female and three male heads. n.s., not significant; $^{*}P < 0.05$; $^{**}P < 0.01$, unpaired *t* test.

elevates dsRNA, we next determined whether similar inflammatory changes result from pan-neuronal heterochromatin decondensation. We find that pan-neuronal RNAi-mediated depletion of *Su(var)205* is sufficient to increase activation of the three major immune pathways (Fig. 7D). *Su(var)205*$^{RNAi}$ increases transcript levels of Toll- and IMD-related antimicrobial peptides, as well as *hop* (the *Drosophila* homolog of human *Jak)* and *Stat92E*, suggesting that the Jak/STAT pathway is activated in response to heterochromatin decondensation in the brain. To further investigate the consequences of heterochromatin decondensation on neuroinflammation, we analyzed the immune response profile of flies with RNAi-mediated depletion of *Su(var)3-9* or *rhino*. We detect significant elevation of transcripts in the Toll, IMD, and Jak/STAT pathways, similar to tau transgenic *Drosophila* (Fig. 7, E and F). Overall, these data provide compelling evidence that the adult *Drosophila* brain mounts an innate immune response as a consequence of genetic manipulations that elevate dsRNA.

## DISCUSSION

Retrotransposon activation is a consequence of physiological aging and pathogenic tau and causally contributes to neurotoxicity (*4*–*7*, *9*, *38*, *39*). In addition, retrotransposons and other repetitive elements are known to form immunogenic dsRNA in various human disorders (*8*, *40*, *41*). In the current study, we link pathogenic tau–induced retrotransposon activation to dsRNA formation by investigating the extent of dsRNA elevation across multiple models of tauopathy as well as the source and mechanism of dsRNA production and consequent neuroinflammation.

We detect significant dsRNA accumulation in postmortem brain tissue from patients with Alzheimer's disease and PSP and in brains of mouse and *Drosophila* models of tauopathy. These findings are consistent with previous reports that cellular detectors of dsRNA such as protein kinase RNA-activated (PKR) are elevated in brains of patients with Alzheimer's disease (*42*–*45*). While dsRNA has never before been analyzed in the context of tauopathy, recent bioinformatic analyses of microglial transcriptomic changes in human Alzheimer's disease, FTD, PSP, and rTg4510 mice propose a model in which tau-induced changes in chromatin structure cause activation of dsRNA receptors to trigger a microglial type I interferon response (*46*). Our finding that dsRNA and MDA5 are elevated in tau-affected brains and that reduction of dsRNA suppresses tau-induced neurotoxicity in *Drosophila* supports a causal link between dsRNA and an innate immune response but points toward astrocytes as a mediator of this effect. It appears that increased dsRNA production is an early event in the course of tau-induced toxicity, as dsRNA is significantly elevated in brains of patients at Braak stage II/III compared to Braak 0, as early as 6 months in brains of rTg4510 tau transgenic mice, and before the exponential decline in survivorship of tau transgenic *Drosophila*. While dsRNA are highly stable RNA species (*40*), we acknowledge that use of postmortem human tissue may present variability due to differences in tissue collection and storage. Our use of a multisystem approach, however, decreases the inherent limitations of any one model system.

Our analyses of tau-affected human, mouse, and *Drosophila* brains reveal significant deposition of dsRNA in astrocytes. Astrocytes provide metabolic support for neurons, regulate neurotransmitters, and maintain blood-brain barrier integrity (*47*). In physiological aging and disease, astrocytes respond to injury and dyshomeostasis of the neuronal environment, a process known as "gliosis" (*48*, *49*). In tauopathies, astrocytes play a key role in responding to pathogenic tau and neurotoxicity (*47*, *50*), and transplantation of isogenic control astrocytes into brains of hTau.P301S mice prevents tau-induced neuronal death (*51*). While *Drosophila* do not have bona fide astrocytes, astrocyte-like glial cells provide similar trophic support to neurons as astrocytes do in vertebrates (*25*). Cultured human astrocytes treated with a dsRNA mimetic up-regulate the dsRNA receptor Toll-like receptor 3 (*52*), indicating that astrocytes respond to extracellular dsRNA. While the astrocytic accumulation of dsRNA in tauopathy suggests that this glial type produces, sequesters, or fails to properly degrade dsRNA in the context of tau pathogenicity, our finding that overexpression of Dicer-2 in neurons of tau transgenic *Drosophila* is sufficient to reduce overall levels of dsRNA supports a model in which retrotransposon transcripts form dsRNA in neurons harboring pathogenic forms of tau and that resulting dsRNA is secreted from neurons and taken up by astrocytes.

Leveraging the fly system, we find that members of the *1731*, *Het-A*, and *Tabor* subfamilies of retrotransposons form dsRNA in brains of tau transgenic *Drosophila*. *1731* and *Tabor* belong to the LTR subclass of retrotransposons (*53*). *Het-A* is a long interspersed nuclear element (LINE)–like non-LTR retrotransposon involved in *Drosophila* telomere maintenance (*54*). While we have previously identified LTR and LINE elements with increased transcript levels in mouse (*5*) and human tauopathy (*6*), we do not currently know

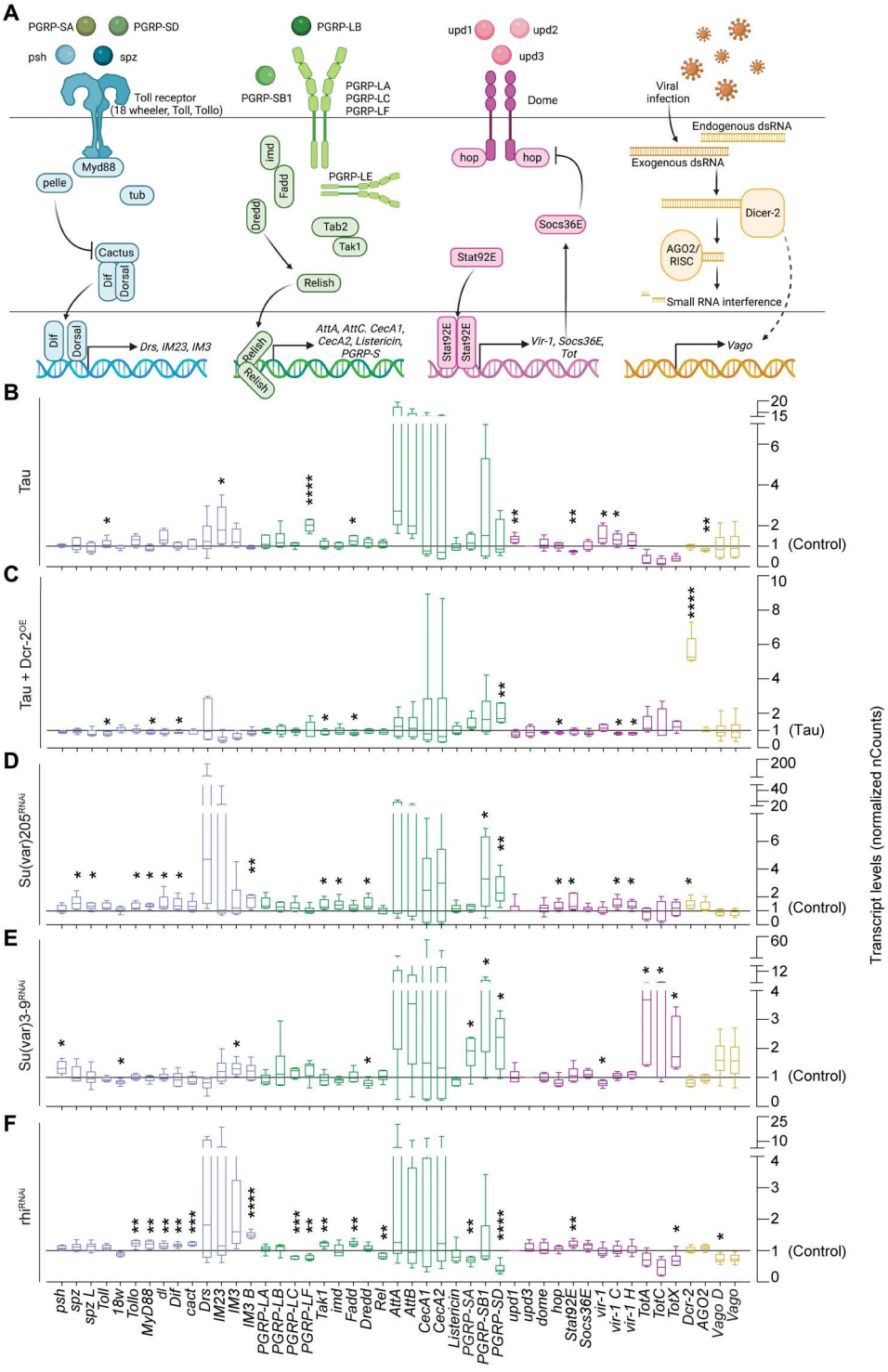


**Fig. 7. Tau- and heterochromatin decondensation–induced elevation of dsRNA are causally associated with innate immune activation.** (**A**) Schematic of the four immune pathways assayed via NanoString for gene expression, illustration created using BioRender.com. A full list of *Drosophila* genes and their human homologs can be found in table S3. PGRP-SA, Peptidoglycan recognition protein SA; Socs36E, Suppressor of cytokine signaling at 36E; Tab2, TAK1-associated binding protein 2; Tak1, TGF-β activated kinase 1. (**B** to **F**) Normalized gene expression counts (nCounts) of innate immune gene transcripts quantified by NanoString gene expression assay using a custom code set. Gene expression is reported for (B) Tau transgenic, (C) Tau + *Dicer-2* overexpression (tau + Dcr-2$^{OE}$), (D) *Su(var)205*$^{RNAi}$, (E) *Su(var)3-9*$^{RNAi}$, and (F) *rhi*$^{RNAi}$ *Drosophila* as compared to control, which was set to one, with the exception of (C), in which transcript levels in tau transgenic *Drosophila* were set to one. Genes are listed by pathway in order from upstream ligand to downstream antimicrobial peptide and color-coded by immune pathway: Toll in blue, IMD in green, Jak/STAT in purple, and RNAi in yellow. $n = 6$ biological replicates; each replicate consists of a pool of three female and three male heads. Code set probe sequences are listed in table S4. *$P < 0.05$; **$P < 0.01$; ***$P < 0.001$; ****$P < 0.0001$, multiple unpaired two-sample $t$ test with Welch correction. AGO2, Argonaute 2.

whether these elements form dsRNA in the context of vertebrate tauopathy. Although our NanoString-based approach to identify dsRNA-forming retrotransposons in brains of tau transgenic *Drosophila* was effective, we acknowledge that this approach is biased toward identifying dsRNA-forming retrotransposon transcripts already known to be overexpressed in tau transgenic *Drosophila*. Furthermore, because our NanoString analyses use a total brain lysate from *Drosophila* heads and because astrocyte-like glia make up a small fraction of cells within the *Drosophila* brain, this approach is likely an underestimation of the magnitude of changes in dsRNA-forming retrotransposon transcripts in astrocyte-like glia of tau transgenic *Drosophila*. In addition, while we have identified retrotransposons that form dsRNA in brains of tau transgenic *Drosophila*, there are a variety of additional endogenous sources of

intracellular dsRNA (*55*) that could contribute to the burden of dsRNA in tauopathy. In future studies in vertebrates, we recommend a more agnostic approach in which dsRNA are isolated from brain tissue via J2 immunoprecipitation and then subject to RNA sequencing.

Mechanistically, we find that RNAi-mediated depletion of heterochromatin regulators impacts dsRNA formation in the *Drosophila* brain. These findings are consistent with previous studies in which tau-induced heterochromatin decondensation drives retrotransposon transcription (*5*, *6*) and work in *Caenorhabditis elegans* demonstrating that global loss of HP1 is sufficient to elevate dsRNA (*56*). Our findings also align with studies of *C9ORF72* expansion in which alterations in H3K9 posttranslational modifications deplete HP1α and drive repetitive element transcription and dsRNA formation (*57*). Our findings are consistent with a model in which tau-induced, retrotransposon-derived dsRNA drive neuroinflammation. We find that genetic overexpression of Dicer-2 ameliorates dsRNA elevation, neurodegeneration, and neuroinflammation in brains of tau transgenic *Drosophila*. Development of new approaches to elevate or deplete transposable element-derived dsRNA would greatly facilitate our ability to assess dsRNA as a therapeutic and anti-inflammatory target in a variety of human disorders that involve dsRNA production.

Our investigation into the effects of heterochromatin decondensation on dsRNA formation included RNAi-mediated depletion of rhino, a protein involved in heterochromatin maintenance that has been extensively characterized in the *Drosophila* germ line (*34*, *58*). We did not expect to detect such substantial effects of *rhino* depletion on dsRNA formation, neurotoxicity, and neuroinflammation, as this factor is expressed at low levels in the adult *Drosophila* brain. Our findings were nevertheless highly significant and consistent with consequences of genetic manipulation of *Su(var)205* and *Su(var)3-9*. To genetically disrupt piRNA-mediated transposon silencing, we reduced overall levels of *piwi* or *aub* in neurons via RNAi and also introduced a loss-of-function mutation in *AGO3*. While neuronal knockdown of *piwi* and *aub* did not elevate dsRNA in the *Drosophila* brain, we do detect significant elevation of dsRNA in the context of AGO3 loss of function. We acknowledge that there is cross-talk between heterochromatin regulators and piRNA biogenesis factors that may underlie the effects of AGO3 loss of function on dsRNA production. For example, studies in the *Drosophila* germ line report a direct interaction between HP1 and piwi (*59*) and also report that mutations in *rhino* are sufficient to deplete piRNAs originating from dual-strand piRNA clusters (*34*). In general, we find that the effects of dysfunctional piRNA control on dsRNA formation are less profound than loss of heterochromatin-mediated silencing. While it remains to be tested, we speculate that piRNAs cannot recognize and bind to these transcripts because of the double-stranded nature of dsRNA.

We find that both pathogenic tau– and RNAi-mediated heterochromatin decondensation are sufficient to drive neuroinflammation in *Drosophila*, with shared induction of the Toll, IMD, and Jak/STAT pathways. An accumulating set of data suggest that retrotransposon activation is consistently immunogenic in a variety of human disorders, a process initiated by the detection of retrotransposon-derived nucleic acids via dsRNA-sensing machinery RIG-I/MDA5, PKR, and adenosine deaminase acting on RNA (ADAR) (*1*, *8*–*11*, *60*). In models of amyotrophic lateral sclerosis (ALS) and cancers such as acute myeloid leukemia, decondensation of LINE elements triggers RIG-I–mediated immune responses (*8*, *11*, *61*). *Alu*- and *LINE*-derived dsRNA initiate innate immune responses in models of Aicardi-Goutières syndrome (AGS) (*10*) and multiple sclerosis (*14*, *37*). In patients with AGS, mutations in *ADAR* result in elevated type I interferon response (*11*), suggesting that deficits in dsRNA editing by ADAR drive inflammation. Similarly, studies in *C9ORF2* ALS-FTD brain find that *C9ORF72*-derived dsRNA accumulates in the cytoplasm of neurons, activates interferon signaling, and mediates cell-autonomous and nonautonomous neuronal death (*40*). In addition, depletion of TAR DNA-binding protein 43 (TDP-43) increases levels of repetitive elements and dsRNA and elevates proinflammatory gene expression-associated dsRNA surveillance proteins (*41*, *56*, *57*, *61*, *62*). These previous reports are consistent with our finding that neuroinflammation in the *Drosophila* brain is in part due to the elevation of dsRNA and support our finding that MDA5-dependent dsRNA surveillance is elevated as a consequence of pathogenic tau accumulation. In the context of recent reports that retrotransposon activation is a feature of pathogenic tau and physiological brain aging (*1*, *4*–*7*, *9*), our findings provide the first evidence, suggesting that neuroinflammatory dsRNA elevation mediated by retrotransposon activation is a feature of Alzheimer's disease, the most common human neurodegenerative disorder, and PSP, a primary tauopathy.

## METHODS

### Postmortem human brain tissue

Human postmortem brain tissue was obtained from the Mayo Clinic Brain Bank (Jacksonville, FL). Deidentified patient information can be found in table S1.

### rTg4510 mouse brain

rTg4510 and nontransgenic control mice (mixed 129S6, FVB genetic background) were obtained from the Jackson Laboratory (IMSR_JAX:024854). Controls harbor the tetracycline-controlled transactivator (tTA) element but lack transgenic human $MAPT^{P301L}$. Female mice were group-housed in a pathogen-free mouse facility on a 12-hour light/dark cycle with ad libitum access to food and water. Following anesthesia with 2% isoflurane, cardiac perfusion was performed with 2× PhosSTOP phosphatase inhibitors (Roche, Indianapolis, IN) and 1× complete protease inhibitors (Roche) in phosphate-buffered saline (PBS) (Thermo Fisher Scientific, Waltham, MA). All experimental procedures in mice were performed according to the National Institutes of Health (NIH) *Guide for the Care and Use of Laboratory Animals*. All mouse experiments were approved by the Institutional Animal Care and Use Committee of the University of Texas MD Anderson Cancer Center.

### *Drosophila* genetics and models

All *Drosophila melanogaster* crosses, stocks, and aging were maintained at 25°C on a 12-hour light/dark cycle with males and females housed in the same vial. Fresh standard diet (Bloomington formulation) was provided every 4 days. Full *Drosophila* genotypes are listed in table S5. All constructs were driven pan-neuronally in *Drosophila* using the galactose-responsive transcription factor (GAL4)/upstream activating sequence (UAS) system with the *elav* promoter driving GAL4 expression. $Su(var)205^{RNAi}$, $rhi^{RNAi}$, $Su(var)3\text{-}9^{RNAi}$, and $aub^{RNAi}$ (*63*) were obtained from the Vienna *Drosophila*

Resource Center (www.vdrc.at). The AGO3$^{LOF}$ and UAS-Dcr-2 stocks were obtained from the Bloomington *Drosophila* Stock Center (NIH P40OD018537).

### Immunofluorescence

For immunofluorescence analyses of postmortem human brain, 10-μm frozen sections were fixed with 4% paraformaldehyde (PFA) for 10 min and ultraviolet photobleached for 4.5 hours at 4°C. Sections were blocked with 2% milk in PBS plus 0.2% Triton-X 100 ($PBS_{Tr}$) for 30 min and incubated with J2 (Scicons/Exalpha Biologicals) and GFAP (Abcam), MAP2 (Millipore), or Iba1 (Wako) antibodies diluted in blocking solution overnight at 4°C. After two washes in $PBS_{Tr}$ and one in PBS, sections were incubated with goat anti-mouse Alexa Fluor 647 and goat anti-rabbit Alexa Fluor 488–conjugated antibodies for 2 hours at room temperature in blocking solution. For detection of MDA5 in GFAP-positive astrocytes, sections were incubated with anti-MDA5 (Abcam) and anti-GFAP (Abcam), followed with goat anti-chicken Alexa Fluor 488 and goat anti-rabbit Alexa Fluor 555–conjugated antibodies. All incubations were performed in a humidified chamber.

Immunofluorescence in mouse tissues was performed on coronal control and rTg4510 mouse MultiBrain sections that were cryoprotected, embedded in a solid matrix, and sectioned at a thickness of 35 μm by Neuroscience Associates Inc. (Knoxville, TN). Following removal from storage and three washes in PBS, floating sections were incubated with J2 and GFAP, MAP2, or Iba1 antibodies overnight at 4°C in a blocking solution of 2% normal goat serum in 1× $PBS_{Tr}$. After three washes in $PBS_{Tr}$, sections were incubated with goat anti-mouse Alexa Fluor 647 and goat anti-rabbit Alexa Fluor 488–conjugated antibodies in blocking solution for 2 hours at room temperature. For detection of MDA5 in GFAP-positive astrocytes, sections were incubated with MDA5 and GFAP antibodies, followed with goat anti-chicken Alexa Fluor 488 and goat anti-rabbit Alexa Fluor 555–conjugated antibodies. Sections were mounted to slides and a coverslip was set with Fluoromount G + DAPI (4′,6-diamidino-2-phenylindole).

For immunofluorescence in flies, *Drosophila* were anesthetized, and whole brains were dissected in PBS and fixed in 4% PFA for 10 min. After blocking with 2% BSA in $PBS_{Tr}$ for 30 min, brains were incubated with J2 anti-dsRNA antibody diluted 1:300 in blocking buffer overnight. After washing twice in $PBS_{Tr}$ and once in PBS, brains were incubated with Alexa Fluor 647 for 2 hours at room temperature. Brains were washed once again as above, and coverslips were mounted with Fluoromount G + DAPI (SouthernBiotech). All incubations were completed in a humidifying chamber. For colocalization experiments, after initial secondary incubation, brains were blocked with 10% normal goat serum diluted in $PBS_{Tr}$. The primary incubation in blocking buffer was repeated for elav and repo with Alex4 Fluor 88– and Alex Fluor 555–conjugated secondary antibodies, respectively. All *Drosophila*, mouse, and human tissue samples were visualized by confocal microscopy (Zeiss 880, Zeiss 780, and Zeiss 710). Image analysis was completed for all immunofluorescence samples using Fiji (NIH). All antibodies and concentrations are listed in table S6.

### Enzyme-linked immunosorbent assay

ELISA was used to detect dsRNA levels as modified from (*13*, *64*–*66*). A 96-well plate was coated overnight at 4°C with 1 μg/μl concentration of the anti-dsRNA antibody J2. The next day, the ELISA plate was washed with wash buffer (1× PBS with 0.5% Tween 20) three times. Following RNA isolation by TRIzol, total RNA of biological replicates of six pooled samples (three males and three females) were loaded in triplicate on the J2-coated ELISA plate and incubated overnight at 4°C. Poly polyinosinic:polycytidylic acid (poly I:C) was used as a standard in each run and loaded in duplicate from a range of 0 to 100 ng/μl. Samples were removed after incubation, and the plate was washed three times with wash buffer. The K2 anti-dsRNA antibody (Scicons/Exalpha Biologicals) was then added to the ELISA plate at a 1:4 dilution and incubated at room temperature for 1 hour. Following three washes with wash buffer, anti-mouse IgM antibody conjugated to alkaline phosphatase (EMD Millipore) was added at a dilution of 1:5000 and incubated for 1 hour. The ELISA plate was washed four times with 1× tris-buffered saline with 0.5% Tween 20, and samples were developed with 100 μg of *p*-nitrophenylphosphate (EMD Millipore).

### Terminal deoxynucleotidyl transferase–mediated deoxyuridine triphosphate nick end labeling

TUNEL-positive neurons in *Drosophila* brains were quantified with the terminal deoxynucleotidyl transferase FragEL kit for TUNEL staining (Calbiochem). Formalin-fixed, paraffin-embedded *Drosophila* heads were sectioned at 4 μm, and staining was completed according to the manufacturer protocol. Secondary detection of biotin-labeled deoxynucleotides at exposed ends of DNA fragments was completed with diaminobenzidine. Bright-field microscopy was used to count TUNEL-positive neurons throughout the entire fly brain.

### Digital polymerase chain reaction

To quantify *rhino* RNA transcripts, six biological samples (six *Drosophila* heads per sample) were homogenized in TRIzol for RNA extraction (Invitrogen). Total RNA concentrations were quantified on a NanoDrop 8000 spectrophotometer (Thermo Fisher Scientific) and 1 μg of RNA was reverse-transcribed (cDNA Reverse Transcription Kit, Applied Biosystems). cDNA was mixed with a *rhino*-specific TaqMan gene expression assay (Thermo Fisher Scientific), loaded on to a digital polymerase chain reaction (PCR) chip, sealed, and amplified. Amplified chips were read and analyzed on the Applied Biosystems QuantStudio 3D Digital PCR system, and the absolute concentration in copies per microliter was determined. The TaqMan gene expression primer and probe for *rhino* was predesigned by Thermo Fisher Scientific.

### RNA isolation and dsRNA immunoprecipitation

RNA was isolated from six pooled heads per genotype, composed of three males and three females, with TRIzol extraction. Total isolated RNA was then used for ELISA and immune gene expression NanoString experiments. For NanoString-based analysis of dsRNA identity, immunoprecipitation of dsRNA was performed on the basis of previously described protocols (*41*, *66*, *67*). Briefly, 10 fly heads per sample were homogenized in radioimmunoprecipitation buffer (50 mM tris-HCL, 0.5% Nonidet-P40, 1.5 mM MgCl, 140 nM NaCl, and 1 mM dithiothreitol) with 1 μg of RNaseOUT (Invitrogen) and precleared with 40 μl of protein A Dynabeads (Invitrogen) for 1 hour at 4°C. After bead clearance, precleared lysate was split in two and diluted to a volume of 200 μl with cold binding buffer (0.0025% Triton X-100 in 1× PBS). Precleared lysate (200 μl) was stored at −80°C for "input." A 1 μg of J2 anti-dsRNA antibody

was added to precleared lysate and incubated at 4°C overnight. After incubation with J2, 50 µl of prewashed protein A Dynabeads were added and incubated for 4 hours at 4°C. Following incubation, the incubated lysate was removed, and beads were washed with cold binding buffer five times. Isolated dsRNA bound to beads and total RNA from input were extracted with TRIzol. All concentrations were measured by Qubit. To ensure that the anti-dsRNA antibody was specific to dsRNA isolation, an antibody control was first performed using mouse IgG2A (Sigma-Aldrich).

### NanoString assays

For NanoString-based analysis of dsRNA identity, the custom retrotransposon code set was based on a slightly modified version of a previous code set developed for the detection of tau-induced retrotransposons (*6*). The retrotransposon code set consists of three internal control genes and 25 probes. A full description of the retrotransposon code set can be found in table S2. Input RNA and dsRNA (50 ng) isolated by J2 immunoprecipitation were hybridized to the retrotransposon code set. For NanoString-based analysis of immune gene expression, the custom immune response code set was designed on the basis of previously identified innate immune genes differentially expressed in tau transgenic *Drosophila* from two independently generated total RNA sequencing datasets (*6*, *68*). The immune response code set consists of probes for 50 innate immune genes, covering all isoforms transcribed and four internal control genes. A full description of the immune response code set can be found in table S4. Following RNA isolation with TRIzol, 10 ng of total RNA was hybridized to the code set as described in the NanoString nCounter XT CodeSet Gene Expression Assay manual. All assays and samples were analyzed following code set hybridization on the SPRINT Digital Analyzer, and normalization was completed using nSolver4 software (NanoString Technologies Inc.).

### Statistical analyses

For all pairwise comparisons, Student's *t* test was used, with Welsh correction for SD where applicable. When performing multiple comparisons, a one-way analysis of variance (ANOVA) with Tukey post hoc test was applied. For NanoString-based analysis of retrotransposon dsRNA, dsRNA and input counts were normalized to the geometric mean of all retrotransposon transcripts across samples, and dsRNA for each retrotransposon were normalized to input for each sample. In all NanoString analyses, a multiple unpaired two-sample *t* test with Welch correction was used. For all statistical tests, a confidence interval of 95% was assumed. G*Power software was used for determining sample size in the dsRNA ELISA. All analyses were performed using Prism8 software (GraphPad). Samples were randomized, and investigators were blinded to genotype in all immunofluorescence when possible.

## Supplementary Materials

**This PDF file includes:**

Figs. S1 to S6

Tables S1 to S6

View/request a protocol for this paper from *Bio-protocol*.

## REFERENCES AND NOTES


1. V. Gorbunova, A. Seluanov, P. Mita, W. McKerrow, D. Fenyö, J. D. Boeke, S. B. Linker, F. H. Gage, J. A. Kreiling, A. P. Petrashen, T. A. Woodham, J. R. Taylor, S. L. Helfand, J. M. Sedivy, The role of retrotransposable elements in ageing and age-associated diseases. *Nature* **596**, 43–53 (2021).
2. S. Lanciano, G. Cristofari, Measuring and interpreting transposable element expression. *Nat. Rev. Genet.* **21**, 721–736 (2020).
3. H. Kaneko, S. Dridi, V. Tarallo, B. D. Gelfand, B. J. Fowler, W. G. Cho, M. E. Kleinman, S. L. Ponicsan, W. W. Hauswirth, V. A. Chiodo, K. Karikó, J. W. Yoo, D. K. Lee, M. Hadziahmetovic, Y. Song, S. Misra, G. Chaudhuri, F. W. Buaas, R. E. Braun, D. R. Hinton, Q. Zhang, H. E. Grossniklaus, J. M. Provis, M. C. Madigan, A. H. Milam, N. L. Justice, R. J. C. Albuquerque, A. D. Blandford, S. Bogdanovich, Y. Hirano, J. Witta, E. Fuchs, D. R. Littman, B. K. Ambati, C. M. Rudin, M. M. W. Chong, P. Provost, J. F. Kugel, J. A. Goodrich, J. L. Dunaief, J. Z. Baffi, J. Ambati, DICER1 deficit induces Alu RNA toxicity in age-related macular degeneration. *Nature* **471**, 325–332 (2011).
4. C. Guo, H.-H. Jeong, Y.-C. Hsieh, H.-U. Klein, D. A. Bennett, P. L. De Jager, Z. Liu, J. M. Shulman, Tau activates transposable elements in Alzheimer's disease. *Cell Rep.* **23**, 2874–2880 (2018).
5. P. Ramirez, G. Zuniga, W. Sun, A. Beckmann, E. Ochoa, S. L. DeVos, B. Hyman, G. Chiu, E. R. Roy, W. Cao, M. Orr, V. Buggia-Prevot, W. J. Ray, B. Frost, Pathogenic tau accelerates aging-associated activation of transposable elements in the mouse central nervous system. *Prog. Neurobiol.* **208**, 102181 (2022).
6. W. Sun, H. Samimi, M. Gamez, H. Zare, B. Frost, Pathogenic tau-induced piRNA depletion promotes neuronal death through transposable element dysregulation in neurodegenerative tauopathies. *Nat. Neurosci.* **21**, 1038–1048 (2018).
7. J. Grundman, B. Spencer, F. Sarsoza, R. A. Rissman, Transcriptome analyses reveal tau isoform-driven changes in transposable element and gene expression. *PLOS ONE* **16**, e0251611 (2021).
8. T. L. Cuellar, A.-M. Herzner, X. Zhang, Y. Goyal, C. Watanabe, B. A. Friedman, V. Janakiraman, S. Durinck, J. Stinson, D. Arnott, T. K. Cheung, S. Chaudhuri, Z. Modrusan, J. M. Doerr, M. Classon, B. Haley, Silencing of retrotransposons by SETDB1 inhibits the interferon response in acute myeloid leukemia. *J. Cell Biol.* **216**, 3535–3549 (2017).
9. M. De Cecco, T. Ito, A. P. Petrashen, A. E. Elias, N. J. Skvir, S. W. Criscione, A. Caligiana, G. Brocculi, E. M. Adney, J. D. Boeke, O. Le, C. Beauséjour, J. Ambati, K. Ambati, M. Simon, A. Seluanov, V. Gorbunova, P. E. Slagboom, S. L. Helfand, N. Neretti, J. M. Sedivy, L1 drives IFN in senescent cells and promotes age-associated inflammation. *Nature* **566**, 73–78 (2019).
10. C. A. Thomas, L. Tejwani, C. A. Trujillo, P. D. Negraes, R. H. Herai, P. Mesci, A. Macia, Y. J. Crow, A. R. Muotri, Modeling of TREX1-dependent autoimmune disease using human stem cells highlights L1 accumulation as a source of neuroinflammation. *Cell Stem Cell* **21**, 319–331.e8 (2017).
11. K. Zhao, J. Du, Y. Peng, P. Li, S. Wang, Y. Wang, J. Hou, J. Kang, W. Zheng, S. Hua, X.-F. Yu, LINE1 contributes to autoimmunity through both RIG-I- and MDA5-mediated RNA sensing pathways. *J. Autoimmun.* **90**, 105–115 (2018).
12. H. Braak, E. Braak, Neuropathological stageing of Alzheimer-related changes. *Acta Neuropathol.* **82**, 239–259 (1991).
13. J. Schönborn, J. Oberstas, E. Breyel, J. Tittgen, N. Schumacher, N. Lukacs, Monoclonal antibodies to double-stranded RNA as probes of RNA structure in crude nucleic acid extracts. *Nucleic Acids Res.* **19**, 2993–3000 (1991).
14. S. Ahmad, X. Mu, F. Yang, E. Greenwald, J. W. Park, E. Jacob, C.-Z. Zhang, S. Hur, Breaching self-tolerance to Alu duplex RNA underlies MDA5-mediated inflammation. *Cell* **172**, 797–810.e13 (2018).
15. S. Hur, Double-stranded RNA sensors and modulators in innate immunity. *Annu. Rev. Immunol.* **37**, 349–375 (2019).
16. M. Hong, V. Zhukareva, V. Vogelsberg-Ragaglia, Z. Wszolek, L. Reed, B. I. Miller, D. H. Geschwind, T. D. Bird, D. McKeel, A. Goate, J. C. Morris, K. C. Wilhelmsen, G. D. Schellenberg, J. Q. Trojanowski, V. M.-Y. Lee, Mutation-specific functional impairments in distinct tau isoforms of hereditary FTDP-17. *Science* **282**, 1914–1917 (1998).
17. K. J. Kopeikina, M. Polydoro, H. C. Tai, E. Yaeger, G. A. Carlson, R. Pitstick, B. T. Hyman, T. L. Spires-Jones, Synaptic alterations in the rTg4510 mouse model of tauopathy. *J. Comp. Neurol.* **521**, 1334–1353 (2013).
18. T. L. Spires, J. D. Orne, K. SantaCruz, R. Pitstick, G. A. Carlson, K. H. Ashe, B. T. Hyman, Region-specific dissociation of neuronal loss and neurofibrillary pathology in a mouse model of tauopathy. *Am. J. Pathol.* **168**, 1598–1607 (2006).
19. K. Santacruz, J. Lewis, T. Spires, J. Paulson, L. Kotilinek, M. Ingelsson, A. Guimaraes, M. Deture, M. Ramsden, E. McGowan, C. Forster, M. Yue, J. Orne, C. Janus, A. Mariash, M. Kuskowski, B. Hyman, M. Hutton, K. H. Ashe, Tau suppression in a neurodegenerative mouse model improves memory function. *Science* **309**, 476–481 (2005).

20. M. Ramsden, L. Kotilinek, C. Forster, J. Paulson, E. McGowan, K. SantaCruz, A. Guimaraes, M. Yue, J. Lewis, G. Carlson, M. Hutton, K. H. Ashe, Age-dependent neurofibrillary tangle formation, neuron loss, and memory impairment in a mouse model of human tauopathy (P301L). *J. Neurosci.* **25**, 10637–10647 (2005).
21. I. J. Hartnell, D. Blum, J. A. R. Nicoll, G. Dorothee, D. Boche, Glial cells and adaptive immunity in frontotemporal dementia with tau pathology. *Brain* **144**, 724–745 (2021).
22. C. W. Wittmann, M. F. Wszolek, J. M. Shulman, P. M. Salvaterra, J. Lewis, M. Hutton, M. B. Feany, Tauopathy in *Drosophila*: Neurodegeneration without neurofibrillary tangles. *Science* **293**, 711–714 (2001).
23. V. Khurana, I. Elson-Schwab, T. A. Fulga, K. A. Sharp, C. A. Loewen, E. Mulkearns, J. Tyynelä, C. R. Scherzer, M. B. Feany, Lysosomal dysfunction promotes cleavage and neurotoxicity of tau in vivo. *PLOS Genet.* **6**, 1–11 (2010).
24. B. Frost, M. Hemberg, J. Lewis, M. B. Feany, Tau promotes neurodegeneration through global chromatin relaxation. *Nat. Neurosci.* **17**, 357–366 (2014).
25. M. R. Freeman, *Drosophila* central nervous system glia. *Cold Spring Harb. Perspect. Biol.* **7**, a020552 (2015).
26. V. Kis, B. Barti, M. Lippai, M. Sass, Specialized cortex glial cells accumulate lipid droplets in *Drosophila melanogaster*. *PLOS ONE* **10**, e0131250 (2015).
27. R. Hilu-Dadia, E. Kurant, Glial phagocytosis in developing and mature *Drosophila* CNS: Tight regulation for a healthy brain. *Curr. Opin. Immunol.* **62**, 62–68 (2020).
28. Y.-H. Chang, R. M. Keegan, L. Prazak, J. Dubnau, Cellular labeling of endogenous retrovirus replication (CLEVR) reveals de novo insertions of the gypsy retrotransposable element in cell culture and in both neurons and glial cells of aging fruit flies. *PLOS Biol.* **17**, e3000278 (2019).
29. Y.-H. Chang, J. Dubnau, The gypsy endogenous retrovirus drives non-cell-autonomous propagation in a *Drosophila* TDP-43 model of neurodegeneration. *Curr. Biol.* **29**, 3135–3152.e4 (2019).
30. S. Deddouche, N. Matt, A. Budd, S. Mueller, C. Kemp, D. Galiana-Arnoux, C. Dostert, C. Antoniewski, J. A. Hoffmann, J.-L. Imler, The DExD/H-box helicase Dicer-2 mediates the induction of antiviral activity in *Drosophila*. *Nat. Immunol.* **9**, 1425–1432 (2008).
31. A. Mussabekova, L. Daeffler, J.-L. Imler, Innate and intrinsic antiviral immunity in *Drosophila*. *Cell. Mol. Life Sci.* **74**, 2039–2054 (2017).
32. L. Fanti, M. Berloco, L. Piacentini, S. Pimpinelli, Chromosomal distribution of heterochromatin protein 1 (HP1) in *Drosophila*: A cytological map of euchromatic HP1 binding sites. *Genetica* **117**, 135–147 (2003).
33. A. B. Eberle, A. Jordán-Pla, A. Gañez-Zapater, V. Hessle, G. Silberberg, A. von Euler, R. A. Silverstein, N. Visa, An Interaction between RRP6 and SU(VAR)3-9 targets RRP6 to heterochromatin and contributes to heterochromatin maintenance in *Drosophila melanogaster*. *PLOS Genet.* **11**, e1005523 (2015).
34. C. Klattenhoff, H. Xi, C. Li, S. Lee, J. Xu, J. S. Khurana, F. Zhang, N. Schultz, B. S. Koppetsch, A. Nowosielska, H. Seitz, P. D. Zamore, Z. Weng, W. E. Theurkauf, The *Drosophila* HP1 homolog Rhino is required for transposon silencing and piRNA production by dual-strand clusters. *Cell* **138**, 1137–1149 (2009).
35. D. Vermaak, S. Henikoff, H. S. Malik, Positive selection drives the evolution of *rhino*, a member of the heterochromatin protein 1 family in *Drosophila*. *PLOS Genet.* **1**, e9 (2005).
36. T. K. Saldi, P. K. Gonzales, T. J. LaRocca, C. D. Link, Neurodegeneration, heterochromatin, and double-stranded RNA. *J. Exp. Neurosci.* **13**, 1179069519830697 (2019).
37. M. J. Heinrich, C. A. Purcell, A. J. Pruijssers, Y. Zhao, C. F. Spurlock III, S. Sriram, K. M. Ogden, T. S. Dermody, M. B. Scholz, P. S. Crooke III, J. Karijolich, T. M. Aune, Endogenous double-stranded Alu RNA elements stimulate IFN-responses in relapsing remitting multiple sclerosis. *J. Autoimmun.* **100**, 40–51 (2019).
38. W. Li, L. Prazak, N. Chatterjee, S. Grüninger, L. Krug, D. Theodorou, J. Dubnau, Activation of transposable elements during aging and neuronal decline in *Drosophila*. *Nat. Neurosci.* **16**, 529–531 (2013).
39. J. G. Wood, B. C. Jones, N. Jiang, C. Chang, S. Hosier, P. Wickremesinghe, M. Garcia, D. A. Hartnett, L. Burhenn, N. Neretti, S. L. Helfand, Chromatin-modifying genetic interventions suppress age-associated transposable element activation and extend life span in *Drosophila*. *Proc. Natl. Acad. Sci. U.S.A.* **113**, 11277–11282 (2016).
40. S. Rodriguez, A. Sahin, B. R. Schrank, H. Al-Lawati, I. Costantino, E. Benz, D. Fard, A. D. Albers, L. Cao, A. C. Gomez, K. Evans, E. Ratti, M. Cudkowicz, M. P. Frosch, M. Talkowski, P. K. Sorger, B. T. Hyman, M. W. Albers, Genome-encoded cytoplasmic double-stranded RNAs, found in *C9ORF72* ALS-FTD brain, propagate neuronal loss. *Sci. Transl. Med.* **13**, eaaz4699 (2021).
41. T. J. LaRocca, A. Mariani, L. R. Watkins, C. D. Link, TDP-43 knockdown causes innate immune activation via protein kinase R in astrocytes. *Neurobiol. Dis.* **132**, 104514 (2019).
42. A. B. Salmina, Y. K. Komleva, O. L. Lopatina, N. V. Kuvacheva, Y. V. Gorina, Y. A. Panina, Y. A. Uspenskaya, M. M. Petrova, I. V. Demko, A. S. Zamay, N. A. Malinovskaya, Astroglial control of neuroinflammation: TLR3-mediated dsRNA-sensing pathways are in the focus. *Rev. Neurosci.* **26**, 143–159 (2015).
43. F. Mouton-Liger, C. Paquet, J. Dumurgier, P. Lapalus, F. Gray, J.-L. Laplanche, J. Hugon; Groupe d'Investigation du Liquide Céphalorachidien Study Network, Increased cerebrospinal fluid levels of double-stranded RNA-dependant protein kinase in Alzheimer's disease. *Biol. Psychiatry* **71**, 829–835 (2012).
44. J. Hugon, F. Mouton-Liger, J. Dumurgier, C. Paquet, PKR involvement in Alzheimer's disease. *Alzheimers Res. Ther.* **9**, 83 (2017).
45. G. Page, A. Rioux Bilan, S. Ingrand, C. Lafay-Chebassier, S. Pain, M. C. Perault Pochat, C. Bouras, T. Bayer, J. Hugon, Activated double-stranded RNA-dependent protein kinase and neuronal death in models of Alzheimer's disease. *Neuroscience* **139**, 1343–1354 (2006).
46. J. E. Rexach, D. Polioudakis, A. Yin, V. Swarup, T. S. Chang, T. Nguyen, A. Sarkar, L. Chen, J. Huang, L. C. Lin, W. Seeley, J. Q. Trojanowski, D. Malhotra, D. H. Geschwind, Tau pathology drives dementia risk-associated gene networks toward chronic inflammatory states and immunosuppression. *Cell Rep.* **33**, 108398 (2020).
47. G. G. Kovacs, Astroglia and tau: New perspectives. *Front. Aging Neurosci.* **12**, 96 (2020).
48. H. Scheiblich, M. Trombly, A. Ramirez, M. T. Heneka, Neuroimmune connections in aging and neurodegenerative diseases. *Trends Immunol.* **41**, 300–312 (2020).
49. M. T. Heneka, M. J. Carson, J. El Khoury, G. E. Landreth, F. Brosseron, D. L. Feinstein, A. H. Jacobs, T. Wyss-Coray, J. Vitorica, R. M. Ransohoff, K. Herrup, S. A. Frautschy, B. Finsen, G. C. Brown, A. Verkhratsky, K. Yamanaka, J. Koistinaho, E. Latz, A. Halle, G. C. Petzold, T. Town, D. Morgan, M. L. Shinohara, V. H. Perry, C. Holmes, N. G. Bazan, D. J. Brooks, S. Hunot, B. Joseph, N. Deigendesch, O. Garaschuk, E. Boddeke, C. A. Dinarello, J. C. Breitner, G. M. Cole, D. T. Golenbock, M. P. Kummer, Neuroinflammation in Alzheimer's disease. *Lancet Neurol.* **14**, 388–405 (2015).
50. M. J. Reid, P. Beltran-Lobo, L. Johnson, B. G. Perez-Nievas, W. Noble, Astrocytes in tauopathies. *Front. Neurol.* **11**, 572850 (2020).
51. M. Sidoryk-Wegrzynowicz, Y. N. Gerber, M. Ries, M. Sastre, A. M. Tolkovsky, M. G. Spillantini, Astrocytes in mouse models of tauopathies acquire early deficits and lose neurosupportive functions. *Acta Neuropathol. Commun.* **5**, 89 (2017).
52. H. Kim, E. Yang, J. Lee, S.-H. Kim, J.-S. Shin, J. Y. Park, S. J. Choi, S. J. Kim, I.-H. Choi, Double-stranded RNA mediates interferon regulatory factor 3 activation and interleukin-6 production by engaging Toll-like receptor 3 in human brain astrocytes. *Immunology* **124**, 480–488 (2008).
53. T. J. McCullers, M. Steiniger, Transposable elements in *Drosophila*. *Mob. Genet. Elements* **7**, 1–18 (2017).
54. S. Cacchione, G. Cenci, G. D. Raffa, Silence at the end: How *Drosophila* regulates expression and transposition of telomeric retroelements. *J. Mol. Biol.* **432**, 4305–4321 (2020).
55. S. Sadeq, S. Al-Hashimi, C. M. Cusack, A. Werner, Endogenous double-stranded RNA. *Non-Coding RNA* **7**, 15 (2021).
56. T. K. Saldi, P. Gonzales, A. Garrido-Lecca, V. Dostal, C. M. Roberts, L. Petrucelli, C. D. Link, The *Caenorhabditis elegans* ortholog of TDP-43 regulates the chromatin localization of the heterochromatin protein 1 homolog HPL-2. *Mol. Cell. Biol.* **38**, e00668-17 (2018).
57. Y.-J. Zhang, L. Guo, P. K. Gonzales, T. F. Gendron, Y. Wu, K. Jansen-West, A. D. O'Raw, S. R. Pickles, M. Prudencio, Y. Carlomagno, M. A. Gachechiladze, C. Ludwig, R. Tian, J. Chew, M. DeTure, W.-L. Lin, J. Tong, L. M. Daughrity, M. Yue, Y. Song, J. W. Andersen, M. Castanedes-Casey, A. Kurti, A. Datta, G. Antognetti, A. McCampbell, R. Rademakers, B. Oskarsson, D. W. Dickson, M. Kampmann, M. E. Ward, J. D. Fryer, C. D. Link, J. Shorter, L. Petrucelli, Heterochromatin anomalies and double-stranded RNA accumulation underlie *C9orf72* poly(PR) toxicity. *Science* **363**, eaav2606 (2019).
58. F. Mohn, G. Sienski, D. Handler, J. Brennecke, The rhino-deadlock-cutoff complex licenses noncanonical transcription of dual-strand piRNA clusters in *Drosophila*. *Cell* **157**, 1364–1379 (2014).
59. B. Brower-Toland, S. D. Findley, L. Jiang, L. Liu, H. Yin, M. Dus, P. Zhou, S. C. R. Elgin, H. Lin, *Drosophila* PIWI associates with chromatin and interacts directly with HP1a. *Genes Dev.* **21**, 2300–2311 (2007).
60. G. Kassiotis, J. P. Stoye, Immune responses to endogenous retroelements: Taking the bad with the good. *Nat. Rev. Immunol.* **16**, 207–219 (2016).
61. E. Y. Liu, J. Russ, C. P. Cali, J. M. Phan, A. Amlie-Wolf, E. B. Lee, Loss of nuclear TDP-43 is associated with decondensation of LINE retrotransposons. *Cell Rep.* **27**, 1409–1421.e6 (2019).
62. M. Prudencio, P. K. Gonzales, C. N. Cook, T. F. Gendron, L. M. Daughrity, Y. Song, M. T. W. Ebbert, M. van Blitterswijk, Y.-J. Zhang, K. Jansen-West, M. C. Baker, M. DeTure, R. Rademakers, K. B. Boylan, D. W. Dickson, L. Petrucelli, C. D. Link, Repetitive element transcripts are elevated in the brain of C9orf72 ALS/FTLD patients. *Hum. Mol. Genet.* **26**, 3421–3431 (2017).
63. G. Dietzl, D. Chen, F. Schnorrer, K.-C. Su, Y. Barinova, M. Fellner, B. Gasser, K. Kinsey, S. Oppel, S. Scheiblauer, A. Couto, V. Marra, K. Keleman, B. J. Dickson, A genome-wide transgenic RNAi library for conditional gene inactivation in *Drosophila*. *Nature* **448**, 151–156 (2007).

64. W. D. Arndt, S. D. White, B. P. Johnson, T. Huynh, J. Liao, H. Harrington, S. Cotsmire, K. V. Kibler, J. Langland, B. L. Jacobs, Monkeypox virus induces the synthesis of less dsRNA than vaccinia virus, and is more resistant to the anti-poxvirus drug, IBT, than vaccinia virus. *Virology* **497**, 125–135 (2016).
65. M. Bokarewa, A. Tarkowski, M. Lind, L. Dahlberg, M. Magnusson, Arthritogenic dsRNA is present in synovial fluid from rheumatoid arthritis patients with an erosive disease course. *Eur. J. Immunol.* **38**, 3237–3244 (2008).
66. Y. Gao, S. Chen, S. Halene, T. Tebaldi, Transcriptome-wide quantification of double-stranded RNAs in live mouse tissues by dsRIP-Seq. *STAR Protoc.* **2**, e100366 (2021).
67. Y. Gao, R. Vasic, Y. Song, R. Teng, C. Liu, R. Gbyli, G. Biancon, R. Nelakanti, K. Lobben, E. Kudo, W. Liu, A. Ardasheva, X. Fu, X. Wang, P. Joshi, V. Lee, B. Dura, G. Viero, A. Iwasaki, R. Fan, A. Xiao, R. A. Flavell, H.-B. Li, T. Tebaldi, S. Halene, m6A modification prevents formation of endogenous double-stranded RNAs and deleterious innate immune responses during hematopoietic development. *Immunity* **52**, 1007–1021.e8 (2020).
68. R. Mahoney, E. Ochoa, P. Ramirez, H. E. Miller, A. Beckmann, G. Zuniga, R. Dobrowolski, B. Frost, Pathogenic tau causes a toxic depletion of nuclear calcium. *Cell Rep.* **32**, 107900 (2020).

**Acknowledgments:** We thank D. Dickson and the Mayo Clinic Brain Bank for providing human brain tissue. Both custom NanoString gene expression code sets were designed in partnership with the Bioinformatics team at NanoString Technologies Inc. (Seattle, WA), including determination of the appropriate parameters for normalization of data from dsRNA IP samples. We thank the UT Health San Antonio Glenn Biggs Brain Bank for use of the NanoString SPRINT Digital Analyzer platform. The elav and repo antibodies were developed by G. M. Rubin and C. Goodman, respectively, and were obtained from the Developmental Studies Hybridoma Bank (DSHB), created by the National Institute of Child Health and Human Development and maintained at The University of Iowa. We thank the Bloomington *Drosophila* Stock Center (NIH P40OD018537) for the AGO3$^{LOF}$ and UAS-Dcr-2 stocks used in this study. UAS-tau$^{R406W}$ was gifted by M. Feany. Confocal microscopy images generated on the Zeiss 710 system were generated in the Core Optical Imaging Facility, which is supported by UT Health San Antonio and NIH-NCI P30CA5417. **Funding:** This study was supported by the National Institute of Neurological Disorders and Stroke RF1 NS112391 (B.F.), the Rainwater Foundation (B.F.), and the National Institute of General Medical Sciences R25 GM095480-06 (E.O. and P.R.). W.J.R. is supported by the Neurodegeneration Consortium, the Belfer Family Foundation, and the Oskar Fischer Project. K.F.B. is the director of the UT Health San Antonio Glenn Biggs Brain Bank, which is supported by the National Institute on Aging (P30AG066546), the Texas Alzheimer's Research and Care Consortium, the Bill and Rebecca Reed Precision Medicine Center, and the Bartell and Mollie Zachry Endowment for Alzheimer Research and Patient Care. **Author contributions:** The study was conceptualized by E.O. and B.F. E.O., E.G., and J.D.M. performed the experiments. E.O. and P.R. completed the data analysis. B.F. and E.O. participated in study design and in figure and manuscript preparation. K.F.B. selected the cases and acquired the human brain tissue. W.J.R. generated and provided the rTg4510 brain tissue. **Competing interests:** The authors declare that they have no competing interests. **Data and materials availability:** All data needed to evaluate the conclusions in the paper are present in the paper and/or the Supplementary Materials.

Submitted 14 April 2022
Accepted 2 December 2022
Published 6 January 2023
10.1126/sciadv.abq5423